# Chapter 3
# Basic Electrical Impedance Tomography


**Richard Bayford**

## 3.1 Introduction

### *3.1.1 Basic Principles*

Electrical impedance tomography (EIT) in its simplest form is based on the use of small alternating electric currents (up to 5 mA rms) flowing between pairs of electrodes placed around or on the region under investigation. The subsequent voltage measurements made at the surface of the imaging domain are processed to produce a map that represents the variation in impedance across the region of interest. The important features to recognize of this imaging technique are that it is based on nonionizing radiation, portable and inexpensive; a typical system can be produced for relatively low cost. The current injected can be a single frequency or varied as in the extension to EIT known as electrical impedance tomographic spectroscopy (EITS). This approach uses a range of frequencies (typically 9.6 kHz to 1.2 MHz) to produce static images of the thorax (Mayer et al. 2005). Frequency ranges greater than this have been reported (10 MHz) for imaging breast and prostate cancers (Murphy et al. 2017; Mahara et al. 2015) where most of the ion flow is within the intercellular region. For thorax imaging, EITS enabled changes in tissue impedance with respect to frequency to be analysed after reconstruction in subjects where the breath was held at maximum inspiration and expiration. The resulting tissue characterization is consistent with an electrical model of the lungs based on the Cole equation (Cole and Cole 1941; Cole 1942), where parameters were related to alveolar structure and composition. One of the first systems developed for use on humans is shown in Fig. 3.1.

R. Bayford (✉)
Biophysics and Engineering, Middlesex University, London, UK
e-mail: r.bayford@mdx.ac.uk



F. Simini, P. Bertemes-Filho (eds.), *Bioimpedance in Biomedical Applications and Research*, https://doi.org/10.1007/978-3-319-74388-2_3

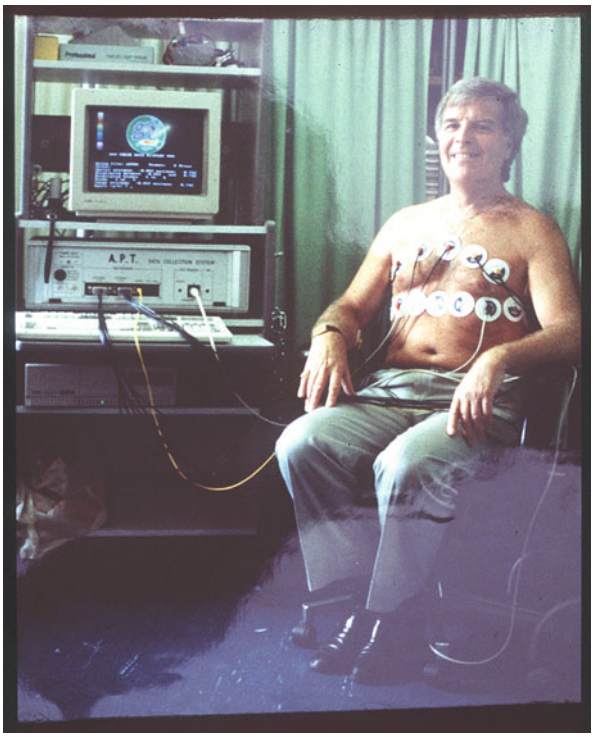


**Fig. 3.1** Chest imaging with the Sheffield Mk 1 system (Provided by Prof Brian Brown)

## 3.2 Hardware

### *3.2.1 Injection Protocols*

The method used to inject current into the domain under investigation can vary. These can be classified as adjacent, opposite and optimum injection pattern assuming the current is injected and voltage is measured, although other variations are possible. The chosen method again depends on the application. For example, when imaging the human brain, the criterion has been to maximize the current density in the brain region. One would assume that an optimum injection pattern would be the choice; however, the complexity of the hardware increases and any errors on each channel that injects current or voltage must be minimized. It is relativity simple to construct an EIT system, but to obtain the dynamic range, accuracy and sample rate that couple with fast change in the physiology is not easily achieved. Another key requirement is the need for these systems to be CE or FDA approved for use on humans, which requires considerable effort.

### *3.2.2 Calibration, Validation and Sources of Error*

There are a number of sources of error in EIT in terms of hardware and image reconstruction. Some of these can be dealt with by improving the hardware design, for example, improving the common-mode rejection ratio (CMRR), thereby reducing the effects of stray capacitance. Many EIT systems apply current or voltage and measure in-phase and quadrature components. It is of key importance that the hardware systems are calibrated to obtain the maximum signal and minimum error. For example, a number of systems are based on one of the earliest systems developed for lunging imaging, known as the Sheffield Mark 1 APT system. This makes serial in-phase voltage measurements and is only used for dynamic images. It uses a constant current generator that is connected to electrodes on the body, usually via a multiplexer, and supplies currents to the object to be imaged. The resulting sinusoidally varying voltage on the surface of the body is sampled on additional electrodes and differentially amplified. The signal can be demodulated by rectification using the reference waveform and filtered to obtain a voltage level that is a measure of the impedance. The principal sources of error in the front end arise from common-mode effects such as skin-electrode problems, contact impedance and stray capacitances. The final error for each measurement is dependent on the complex interaction of these effects and will differ for each electrode combination. New approaches are being developed to overcome these problems using active electrodes (Wu et al. 2016).

## 3.3 Imaging

EIT can produce images that are physiologically useful; however images on their own can have limitations. The image needs to provide full information in regard to the clinical state of the patient in terms of clinical parameters and care need. Two types of image can be produced. The first of these is known as difference imaging, where a change in ratio or percentage represents some physiological parameter like blood volume or volume of air in the lung. The Sheffield Group produced the first lung images using this method, and other systems still provide this type of image, for example, Swisstom AG (Fig. 3.2) and Draeger. The images are obtained by measuring two data sets at different times.

A system that can produce image based on different frequencies at the boundary of the object has also been developed. The difference between two frequencies is divided by a reference data set resulting in frequency difference images. The second type of image that can be obtained is known as absolute imaging, which produces a representation of the absolute conductivity or permittivity used in applications such as breast imaging. This absolute method of imaging is technically more difficult than the difference method, as the contact impedance of the electrodes cannot be accurately characterized when making clinical measurements.

**Fig. 3.2** Swisstom AG EIT system (Images kindly provided by Swisstom AG (http://www.swisstom.com/))

It should be noted that changes in conductivity anywhere in the domain can affect all measurements, not just those on a direct path. In the early days of EIT development, assumptions were made to simplify the mathematics of the reconstruction process, though this assumption limits the accuracy of the reconstructed images. A simple so-called back project algorithm was developed based on the Radon transform used in CT imaging. The back-projection algorithm was developed by Barber and Brown (1984), Barber (1989) for the original Sheffield EIT system and has seen numerous variants and improvements. Another assumption sometimes used, which again was an analogue of those used in CT scanning, was the idea that current path was in a single plane and one could assume a 2D solution would be acceptable. However, as ionic current flows in 3D, then it is essential to develop a 3D solution rather than trying to fit a 2D solution into a 3D problem. A key development to overcome this issue, along with the goal of having a so-called gold standard algorithm based on a consensus linear reconstruction algorithm for lung EIT, has been named GREIT (Graz consensus Reconstruction algorithm for EIT) (Adler et al. 2009). A unified approach to linear image reconstruction has been developed for GREIT. The framework for the linear reconstruction algorithm consists of three points, detailed finite element models of a representative adult and neonatal thorax, a consensus on the performance figures of merit for EIT image reconstruction and a systematic approach to optimize a linear reconstruction matrix to the desired performance measures. In achieving the figures of merit, the requirements in order of importance are (a) a uniform amplitude response, (b) a small and uniform position error, (c) small ringing artefacts, (d) a uniform resolution, (e) limited

shape deformation and (f) high resolution. Such figures of merit must be attained while maintaining small noise amplification and small sensitivity to electrode and boundary movement. The approach represents the consensus of a large and representative group of experts in EIT algorithm design and clinical applications for pulmonary monitoring. GEIT is designed for lung measurements and the above requirements may vary for other clinical applications.

The EIT community has also developed a resource known as EIDORS: electrical impedance tomography and diffuse optical tomography reconstruction software. It is an open source software suite for image reconstruction in electrical impedance tomography and diffuse optical tomography, designed to facilitate collaboration, testing and research in both electrical and optical tomography (Adler and Lionheart 2006).

EIT is governed by the Maxwell equations model (some time termed the full model) as a forward model, with many assumptions used to simplify this. However, some research has been developed to formulate the problem in terms of the Maxwell equations expressed in scalar and vector potentials. This approach leads to boundary conditions that naturally align with the quantities measured by EIT instrumentation. The effect of frequency on the field distribution is illustrated using the high-frequency model and is compared with Laplace solutions. Numerical simulations and experimental results are also presented to illustrate image reconstruction over a range of frequencies using the new implementation. The results show that scalar/vector potential reconstruction produces images which are essentially indistinguishable from a Laplace algorithm for frequencies below 1 MHz but superior at frequencies reaching 10 MHz (Soni et al. 2006).

Traditionally, image reconstruction has been based on Laplace's equation. However, at high frequencies the coupling between electric and magnetic fields requires solution of the full Maxwell equations (Barber and Brown 1984), which are shown below in the simplified approach. The first of these is to assume the reconstruction is quasistatic. This means that the effect of magnetic induction can be ignored in Maxwell's equations so that the governing equations across a medium can be defined as:

$$\nabla \left(\sigma + i\omega\varepsilon\right) \nabla\phi = 0 \tag{3.1}$$

where $\sigma$ is the electric impedance of the medium, $\phi$ is the electric potential, $\omega$ is the frequency and $\varepsilon$ is the electric permittivity. Equation 3.1 can be reduced to the standard governing equation for EIT when we assume that a low frequency or a direct current is used which would be the case in human applications:

$$\nabla \cdot (\nabla\sigma\phi) = 0 \tag{3.2}$$

This can be considered as determining the conductivity distribution from the measurements made at the surface of the domain. For voltage measurements made at the surface of the head, the reconstruction problem can be defined as

$$V = A\sigma \tag{3.3}$$

where $A$ is known as the sensitivity matrix which relates voltages to image pixels. The sensitivity matrix can be considered as the Jacobian of the forward mapping (matrix of partial derivatives). The inverse problem, to find $\sigma$ given $A$ and $V$, becomes $\sigma = A^{-1}\ V$ where $A^{-1}$ is the inverse of $A$ and can be found by a number of methods. However, approximations are sometime used to reduce complexity and computational time of $A$ the forward problem. For example, for analytical brain applications, by assuming the head to be a homogeneous sphere, this does not use accurate geometrical information regarding the shape of the human head and so will introduce errors in the solution.

The aim is to obtain an accurate solution to the forward problem by incorporating the shape and the structure of the boundary form and hence obtain an improved estimation of the values of the elements in the sensitivity matrix $A$. The reconstruction algorithm involves a solution to the forward and inverse problems. The forward problem can be solved in two ways. The first is analytical, for which a number of solutions are available (Bayford 2006; Kolehmainen et al. 1999); the second is by the use of numerical methods like FEM or boundary element method (BEM) (Pidcock et al. 1995a). The analytical methods are preferable as computation time is reduced, but these have been of limited practical value because solutions only exist for a small number of idealized geometries (Pidcock et al. 1995b; Menin et al. 2013).

Table 3.1 gives examples of approaches used to solve the forward problem.

There are a number of approaches to finding a solution to the inverse problem which is ill-posed and can be linear or nonlinear. Many are based on linearization and regularization as in the GREIT algorithm; however if computation limitation is not an issue, then it is possible to achieve a nonlinear solution. Typically for a linear approach to solving the inverse problem, the truncated singular value decomposition (Penrose-Moore pseudo inversion) or Tikhonov regularization is commonly used. Nonlinear approaches are a much wider choice, such as Gauss–Newton, Global Convergence using first-order Taylor expansion approximation, Levenberg–Marquardt involving a second-order Taylor expansion regularized approximation, variable metric with Brent line search using a Hessian's inverse gradual approximation and Newton types and conjugate gradients Polak-Ribiere, with Brent line

**Table 3.1** Examples to solve the forward problem

| | Real | Complex |
|---|---|---|
| Preconditioner | Incomplete Cholesky or algebraic multigrid (Borsic and Bayford 2010) | Incomplete LU (Jehl et al. 2015) |
| Solver | Preconditioned conjugate gradients (PCG) (Borsic et al. 2010) | Bi-conjugated gradients (BiCG) (Dehghani et al. 2005) or generalized minimal residual (GMRES) (Horesh 2006) |

search and regularized search direction—residual error minimization by conjugated search directions (Krylov space) (Lionheart et al. 2004).

None of these methods are ideal; conjugate gradient has the disadvantage that it requires many more iterations than Newton-based algorithms. A line search has to be implemented and scaling should be carefully treated. Newton–Raphson/Gauss–Newton requires assumptions. The forward solution has continuous first and second derivatives in the data and image domains. The benefits of the approach are the fast convergence and easy implementation, but the disadvantage is repeated computation of Cholesky decomposition of a large dense sensitivity matrix. It requires first and second derivatives, and the system matrix is not necessarily symmetric and positive definite away from the solution, which could cause convergence failure. Levenberg–Marquardt benefits are faster convergence and easy implementation, and the solution can be refined due to proper adjustment of the regularization coefficient. However, it requires repeated computation of Cholesky decomposition of a large dense sensitivity matrix which needs first and second derivatives. The system matrix is not necessarily symmetric and positive definite away from the solution which could cause convergence failure.

New methods are still being developed, for example, D-bar (Hamilton 2017) methods solve the nonlinear problem directly, bypassing the need for detailed and time-intensive forward models, to provide absolute (static) as well as time-difference EIT images. It is possible to use coupling the D-bar methodology with the inclusion of high confidence a priori data results in a noise-robust regularized image reconstruction method (Hamilton 2017). This is the first time a priori D-bar method for complex admittivities for absolute imaging has been used. Additionally, the method can be adjusted for, and tested on, time-difference imaging scenarios. The ability of the method to be used for conductivity, permittivity and absolute as well as time-difference imaging provides the user with great flexibility without a high computational cost. More details on the EIT Reconstruction Algorithms: Pitfalls, Challenges and Recent Developments can be found in Lionheart's paper (Lionheart 2004).

It is worth noting that the electrode model is of key importance in both the image reconstruction and the hardware. At present, we do not have a model that satisfies the requirements of the image reconstruction and the hardware. Mathematical models, like the complete electrode model, are used to develop the reconstruction algorithms, but estimating the load impedance on the current deriver is addressed by using equivalent SPICE models. Ideally a model needs to be developed to address both requirement of the imaging and hardware.

## 3.4 EIT Systems

Most EIT systems are developed for specific clinical use, for example, the Dartmouth system is designed for breast imaging and is shown in Fig. 3.3.

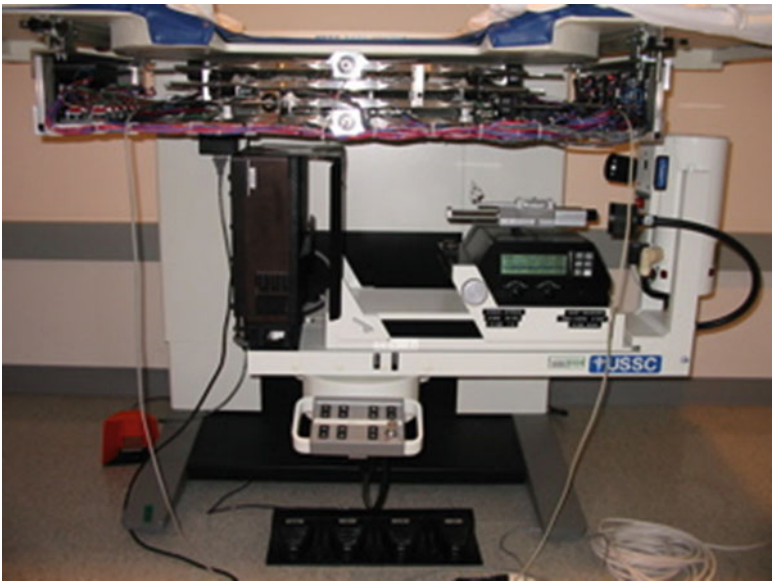


**Fig. 3.3** Dartmouth breast imaging system (Image supplied by Prof Alexander Hartov)

Also there are a number of variations which combine EIT with other modalities, for example, magnetic resonance electrical impedance tomography (MREIT) which aims to improve the limitation of EIT (Fig. 3.4).

## 3.5 Clinical Applications

EIT in its various forms has been applied to a wide range of clinical applications with varying degrees of success. These include thoracic, gastrointestinal function, breast tumour localization and brain function. Those areas that are showing the most promising results are the brain, breast, gastrointestinal tract, lung, rectum and prostate, though only one is getting close to clinical use.

### *3.5.1 Pulmonary Function*

One of the key areas that shows resurgence is monitoring pulmonary function, which was first developed by the Sheffield Group (Barber and Brown 1984). Although there are many other imaging approaches, such as planar X-ray, X-ray CT, MRI and radioisotope scintigraphy, that can all be used to monitor static images of pulmonary function with high spatial resolution so providing information on

**Fig. 3.4** Korean MREIT system (Image supplied by Prof EJ Woo)

ventilation and perfusion. The patient must be brought to the device and repeatedly exposed to radiation with imaging modalities that require the use of X-rays, which is undesirable. MRI offers the advantage that it does not use ionizing radiation; however, as in the case with all the above methods, the subject must be stationary and MRI is considerably more costly. There has been considerable interest in the development of EIT for imaging ventilation and detection of blood clots in the lungs or pulmonary emboli, a common and often serious complication of surgery. Thoracic EIT examinations have been shown to track changes in regional lung volumes at scan rates of up to 40–50 scans/s. It may also be used to monitor the drainage of a pneumothorax caused by pulmonary lesions because the impedance of air is very high, providing high contrast with the surrounding tissue. It has even been used during parabolic flights to determine regional ventilation and fluid shift signals in lateral posture during normo-, hyper-, and microgravity. However, one problem is that as well as being sensitive to lung impedance changes, the technique is also sensitive to the ribs and to tissue movement, which can be large sources of artefact.

EIT also shows promise as a valuable tool for bedside data-driven EIT lung tissue classification for monitoring of mechanically ventilated patients in the intensive care unit (ICU) (Wolf and Arnold 2006). They use a system marketed originally by Viasys (now CareFusion) which is based on the Sheffield Mk1 (Barber and Brown 1984). Lung applications have continued to be developed, for example, Draeger developed clinical systems; these are capable of looking at positive end-expiratory pressure (PEEP). Setting the optimal level of PEEP in the ICU is still considered a

matter of debate. Talmor et al. (2008) used the transpulmonary pressure calculated from the oesophageal balloon to set PEEP in a recent randomized controlled study. This strategy aims at preventing alveolar collapse by counterbalancing the gravitational force of the lung by an equal or higher PEEP. They have evaluated the relation between ventilation distribution measured by EIT and transpulmonary pressure during a PEEP trial in porcine acute lung injury (ALI).

A key area, which is of growing interest, is the need to monitor babies born prematurely where many suffer from respiratory failure due to immaturity of the lung (respiratory distress syndrome, RDS) and lack of control of breathing. Although respiratory support, especially mechanical ventilation, can improve their survival, it also causes severe injury to the vulnerable lung resulting in severe and chronic pulmonary morbidity lasting into adulthood. Electrical impedance tomography (EIT) is the only technology that is available to address this need as well as being cost-effective. EIT has a high temporal resolution (real-time continuous imaging of dynamic lung function), is radiation-free and can be used at the bedside. Another advantage, which is unique, is the patient can move during imaging (cradlproject.org). For EIT to be of clinical relevance, it is important that it can be used reliably by operators with minimal training and display standardized, clinically meaningful results.

A number of research groups have developed hardware systems for research into the use of EIT for pulmonary function, for example, Rensselaer, New York. The adaptive current tomography (ACT) system imaged a simulated pulmonary embolus in a dog, where the first one lung at a time was ventilated and then a major branch of the pulmonary artery was occluded. The region of the lungs that was ventilated but not perfused by blood had different electrical properties and, therefore, was observable in a time-varying conductivity map of the thorax. This group also reconstructed conductivity changes during lung ventilation in human volunteers using a ring of electrodes placed around the thorax and a $4 \times 4$ rectangular array placed on the subject's chest (Gisser et al. 1988).

Swisstom AG has developed a CE clinical EIT system for adults, using a belt that that can be easily applied. They are also working on a system for neonates as part of an EU CRADL project (cradlproject.org). Disorders ranging from lung growth, maturation and control of breathing are among the most important problems faced by the neonatologist. Premature birth occurs in 5–10% of all pregnancies and is frequently accompanied by complications due to lung immaturity. Many preterm infants exhibit lung dysfunction characterized by arrested lung development and interrupted alveolarization. This immature lung phenotype accounts for 75% of early mortality and long-term disability in infants delivered prematurely. Despite improved survival of extremely premature (EP) infants, i.e. those born <27w gestational age (GA), the prevalence of chronic lung disease in infancy has remained high over the last decade. Chronic lung disease of infancy (CLDI) is associated with long-term, and possibly life-long, respiratory morbidity. Objective, non-invasive measures of lung maturity and development, oxygen requirements and lung function, suitable for use in small, unsedated infants, are urgently required to define the nature and severity of persisting lung disease and to identify risk factors for

developing chronic lung problems. Recent progress with EIT has made pulmonary function testing available for this age range and opened up new possibilities for monitoring changes in disease processes affecting the respiratory system. This may improve medical management of infants and children with lung and heart diseases, including those requiring intensive care.

### *3.5.2 Breast Imaging*

Early detection and treatment of tumours in the breast still remains the best method to increase chance of survival among patients. The properties of many tumours, in particular those exhibiting malignancy, differ significantly from the surrounding tissue, and separation and characterization of contrasting tissues can deliver early diagnosis. At present, women are screened for breast cancer using X-ray mammography (MG), although some cancers of the breast cannot be seen using this technique and there are restrictions of the groups of patient that can undergo regular scanning. During this procedure, their breast is compressed flat to visualize all the tissue and minimize the required radiation dose, which can be uncomfortable and sometimes painful for the patient. Another disadvantage of the technique is the high (40%) false-positive rate. A positive test is highly alarming and requires the patient to undergo further testing, which could include fine-needle aspiration or biopsy. Meanwhile, the false-negative rate is 26%. Regular screening is recommended for women over 40 years old, but the technique is difficult with younger women whose breast tissue is generally denser. In a study at Dartmouth College, USA, participants lay prone on a customized table where up to four rings consisting of 16 radially adjustable electrodes are put into contact with the pendant breast. In 6 out of 26 subjects who had ACR 4–5 suspicious lesions, inspection of EIS images using visual criteria resulted in 83% detection specificity and numerical criteria 67% (Bayford and Tizzard 2012). An example is shown in Fig. 3.5.

### *3.5.3 Brain Imaging*

There is also potential for imaging aspects of brain function; the first application is in focal epilepsy which is a functional abnormality often related to a causal structural abnormality, for example, a lesion, and an individual seizure always originates from the same cerebral focus. Patients with intractable epilepsy can require surgery to remove that part of the brain, and accurate localization of the epileptic focus is crucial before surgical excision. The repetitive activity owing to a focal seizure can cause local ischemia, detectable using EIT (Pidcock et al. 1995a). Continuous monitoring is necessary because the occurrence of seizures is so unpredictable; therefore, EIT may be better suited than MRI for localization of epileptic foci. EEG inverse dipole modelling has been tried for this purpose but was not adopted on

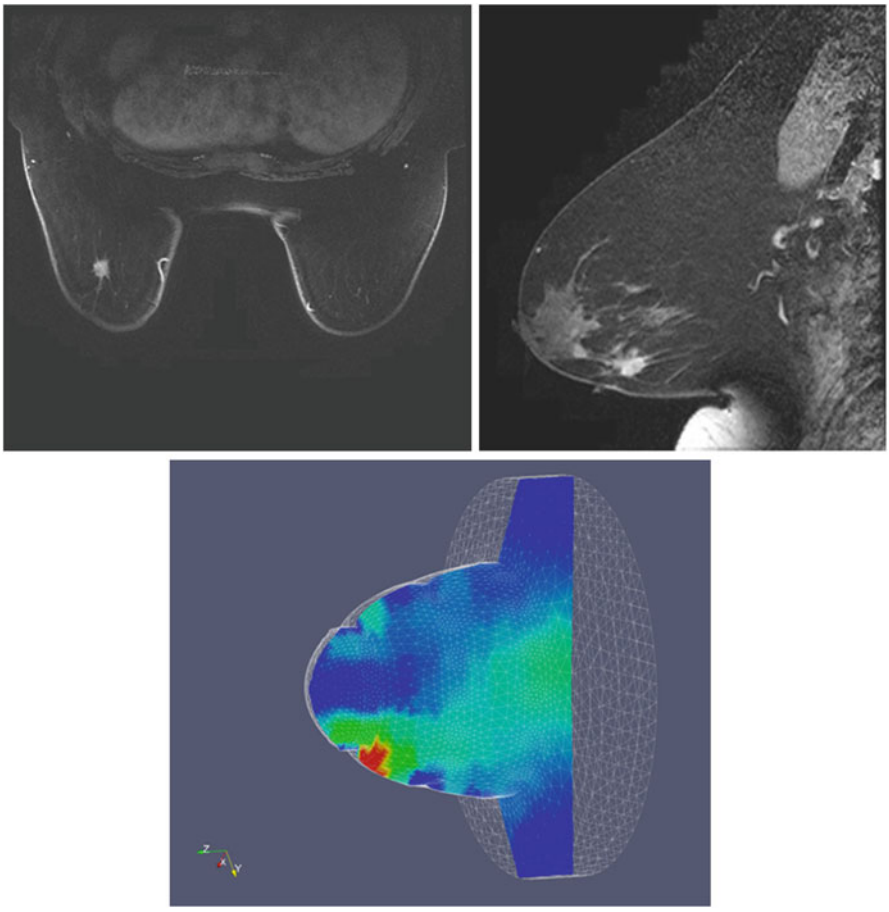

**Fig. 3.5** Contrast-enhanced MR images, 1.3 cm cancerous mass, 5 cm from the nipple, axial, sagittal planes and EIT reconstruction

its own, and a combined set of methods is normally undertaken including MEG. Patients have their epilepsy-suppressing medication suspended for a week prior to surgery, during which time they are monitored with EEG to gain as much electrical information as possible during seizure activity. A technique known as telemetry is quite successful for localization of superficial foci, but less so for foci situated deeper in the brain. For these, EEG electrodes are often implanted deep in the brain, a process that can cause irreversible damage. EIT may provide a more powerful, as well as less invasive, alternative for their localization. An example of this is the use of 31 electrodes applied to the scalp in the same way as in EEG, based on the standard 10–20 configuration with some additional electrode positions. Two hundred and fifty-eight individual voltage measurements were taken to produce one impedance tomogram (Fig. 3.6). Studies have also shown changes of the order of

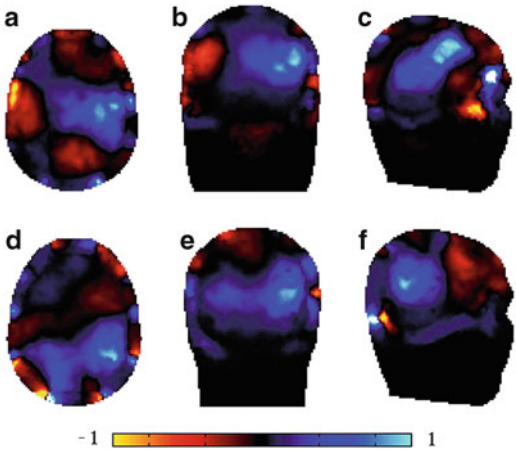


**Fig. 3.6** Reconstructions of data collected approximately 6 s prior to two right temporal complex partial seizures in patient 1. In both cases, three orthogonal planes are shown through the maximum conductivity increase. The axial slices (**a**) and (**f**) are 8 and 21 mm, respectively, above the $z = 0$ plane; the coronal slices (**b**) and (**e**) are −44 and −61 mm, respectively, from $y = 0$; and the sagittal slices (**c**) and (**f**) are 57 and 44 mm, respectively, from $x = 0$ (1)

0.5–1.0% were observed in the raw voltage data during visual evoked responses in healthy volunteers (Bayford and Tizzard 2012; Tidswell et al. 2001).

### *3.5.4 Hyperthermia*

Hyperthermia, which offers the possibility of reducing tumour size, can be used for certain malignancies by applying temperature treatment. This involves concentrated heating of the tumour tissue to approximately 47 °C without damaging the surrounding tissue. EIT has the potential to be useful in this application. However, it has been found that there are artefacts in the resistance images owing to other physiological factors and that they are significant compared with the temperature-dependent changes. The feasibility of EIT for thermometry has also been questioned in light of changes in tissue fluid content during hyperthermic treatment and of the different impedance spectra of skeletal muscle and tumour tissue in rats during this approach (Paulsen et al. 1996).

### *3.5.5 Gastrointestinal*

EIT of gastrointestinal function has also had some success in imaging changes in gastric emptying which can be an indicator of many functional disorders of the gastrointestinal tract, e.g. pyloric stenosis, and of stress. Also, slow gastric emptying can be a problem in the management of newborn babies recovering from intensive care (Bayford and Tizzard 2012).

## 3.6 Variations of EIT

There is an increased interest in a number of new variations on EIT. Two approaches are currently being developed, and though they are a long way from clinical applications, considerable progress is being made in their development. The first is based on the principle of using another image modality combined with EIT, and the second makes use of non-contacting methods using electrical inductors to induce the current or measure the field.

### *3.6.1 Magnetic Resonance Electrical Impedance Tomography*

The first variation is a combination of MRI and EIT known as MREIT. In MREIT, a reconstruction of the cross-sectional current density and conductivity (or resistivity) images of human body with high spatial and contrast resolution can be obtained. Using LF-MRCDI (low-frequency magnetic resonance current density imaging) technique where MR images are acquired with external current injection through surface electrodes, the first images obtained are of internal magnetic flux density distribution. This internal information transforms the ill-posed inverse problem of EIT into a well-posed one in MREIT (Kim et al. 2009).

### *3.6.2 Magnetic Induction Tomography*

The second of these variations on EIT is known as magnetic induction tomography (MIT). In principle, this can detect very small changes using planar gradiometers (PGRAD), low-noise amplifiers and digital signal processing for achieving high SNR. Systems like Gaze (Scharfetter et al. 2005) currently use one single excitation coil (EXC). The sample is rotated in 16 steps of 22.5°. The main advantages of this approach are that the boundary shape is well defined and, because there are no electrodes, the effect of contact impedance is eliminated.

## 3.7 Summary

In conclusion, until a sufficient level of investment is devoted to the development of improving both hardware and reconstruction algorithms, EIT will remain a research tool. This is not to say that it does not have the capability to produce useful clinical results; this review has illustrated a number of these such as continuous monitoring of lung functison and breast tumour localization. However, equipment developed on limited resources cannot hope to achieve the results obtained by other imaging

modalities, such as MRI. EIT also needs to produce useful clinical parameters and not simply images. However, there are promising areas, which are emerging, which could see EIT been adopted in the clinical enrolment (Bayford and Tizzard 2012).

## References


Adler, A., Arnold, J. H., Bayford, R., Borsic, A., Brown, B., Dixon, P., et al. (2009). GREIT: A unified approach to 2D linear EIT reconstruction of lung images. *Physiological Measurement, 30*(6), S35–S55. https://doi.org/10.1088/0967-3334/30/6/S03. Epub 2009 Jun 2.

Adler, A., & Lionheart, W. R. B. (2006). Uses and abuses of EIDORS: An extensible software base for EIT. *Physiological Measurement, 27*(5), S25.

Barber, D. C. (1989). A review of image reconstruction techniques for electrical impedance tomography. *Medical Physics, 16*, 162–169.

Barber, D. C., & Brown, B. H. (1984). Applied potential tomography. *Journal of Physics E: Scientific Instruments, 17*, 723–733.

Bayford, R., & Tizzard, A. (2012). Bioimpedance imaging: An overview of potential clinical applications. *Analyst, 137*(20), 4635–4643. https://doi.org/10.1039/C2AN35874C

Bayford, R. H. (2006). Bioimpedance tomography (electrical impedance tomography). *Annual Review of Biomedical Engineering, 8*, 63–91.

Borsic, A., & Bayford, R. (2010). Forward solving in electrical impedance tomography with algebraic multigrid wavelet based preconditioners. *Journal of Physics: Conference Series, 224*(1), 012053.

Borsic, A., Halter, R., Wan, Y., Hartov, A., & Paulsen, K. D. (2010). Electrical impedance tomography reconstruction for three-dimensional imaging of the prostate. *Physiological Measurement, 31*(8), S1–16. https://doi.org/10.1088/0967-3334/31/8/S01

Cole, K. S. (1942). Dispersion and absorption in dielectrics II. Direct current characteristics. *The Journal of Chemical Physics, 10*, 98. https://doi.org/10.1063/1.1723677

Cole, K. S., & Cole, R. H. (1941). Dispersion and absorption in dielectrics I. Alternating current characteristics. *The Journal of Chemical Physics, 9*, 341. https://doi.org/10.1063/1.1750906

Dehghani, H., Soni, N., Halter, R., Hartov, A., & Paulsen, K. D. (2005). Excitation patterns in three-dimensional electrical impedance tomography. *Physiological Measurement, 26*, S185–S197. https://doi.org/10.1088/0967-3334/26/2/018

Draeger. https://www.draeger.com/en_uk/Hospital/Productselector/Ventilation-and-Respiratory-Monitoring/ICU-Ventilation-and-Respiratory-Monitoring.

Gisser, D. G., Isaacson, D., & Newell, J. C. (1988). Current topics in impedance imaging. *Clinical Physics and Physiological Measurement, 9*, 35.

Hamilton, S. J. (2017). EIT Imaging of admittivities with a D-bar method and spatial prior: Experimental results for absolute and difference imaging. Published 22 May 2017. Institute of Physics and Engineering in Medicine. Physiological Measurement, Volume 38, Number 6. In: *16th International Conference on Electrical Bioimpedance and 17th International Conference on Biomedical Applications of Electrical Impedance Tomography* (pp. 19–23). Stockholm.

Horesh, L. (2006). *Some novel approaches in modelling and image reconstruction for multi-frequency electrical impedance tomography of the human brain*. PhD thesis. London: University College London.

Jehl, M., Dedner, A., Betcke, T., Aristovich, K., Klofkorn, R., & Holder, D. (2015). A fast-parallel solver for the forward problem in electrical impedance tomography. *IEEE Transactions on Biomedical Engineering, 62*(1), 126–137.

Kim, H. J., Kim, Y. T., Minhas, A. S., Jeong, W. C., Woo, E. J., Seo, J. K., et al. (2009). In vivo high-resolution conductivity imaging of the human leg using MREIT:

The first human experiment. *IEEE Transactions on Medical Imaging, 28*, 1681–1687. https://doi.org/10.1109/TMI.2009.2018112

Kolehmainen, V., Arridge, S. R., Lionheart, W. R. B., Vauhkonen, M., & Kaipio, J. P. (1999). Recovery of region boundaries of piecewise constant coefficients of an elliptic PDE from boundary data. *Inverse Problems, 15*(5), 1375.

Lionheart, W., Polydorides, N., & Borsic, A. (2004). Part 1 of electrical impedance tomography: Methods, history and applications. In D. Holder (Ed.), (pp. 3–64). Bristol: Institute of Physics Publishing. ISBN: 0750309520.

Lionheart, W. R. B. (2004). EIT reconstruction algorithms: Pitfalls, challenges and recent developments. *Physiological Measurement, 25*(1), 125.

Mahara, A., Khan, S., Murphy, E., Schned, A., Hyams, E., & Halter, R. J. (2015). 3D microendoscopic electrical impedance tomography for margin assessment during robot-assisted laparoscopic prostatectomy. *IEEE Transactions on Medical Imaging, 34*(7), 1590–1601. https://doi.org/10.1109/TMI.2015.2407833

Mayer, M., Brunner, P., Merwa, R., & Scharfetter, H. (2005). Monitoring of lung edema using focused impedance spectroscopy: A feasibility study. *Physiological Measurement, 26*, 185–192. https://doi.org/10.1088/0967-3334/26/3/004

Menin, O. H., Rolnik, V., & Martinez, A. S. (2013). Boundary element method and simulated annealing algorithm applied to electrical impedance tomography image reconstruction. *Revista Brasileira de Ensino de Física, 35*(2), 1–7.

Murphy, E. K., Mahara, A., Wu, X., & Halter, R. J. (2017). Phantom experiments using soft-prior regularization EIT for breast cancer imaging. Published 22 May 2017, Institute of Physics and Engineering in Medicine. Physiological Measurement, Volume 38, Number 6. In: *16th International Conference on Electrical Bioimpedance and 17th International Conference on Biomedical Applications of Electrical Impedance Tomography* (pp. 19–23). Stockholm.

Paulsen, K. D., Moskowitz, M. J., Ryan, T. P., Mitchell, S. E., & Hoopes, P. J. (1996). Initial in vivo experience with EIT as a thermal estimator during hyperthermia. *International Journal of Hyperthermia, 12*, 573–591. https://doi.org/10.3109/02656739609027666

Pidcock, M. K., Kuzuoglu, M., & Leblebicioglu, K. (1995a). Analytic and semi-analytic solutions in electrical impedance tomography: I. Two-dimensional problems. *Physiological Measurements, 16*, 77–90.

Pidcock, M. K., Kuzuoglu, M., & Leblebicioglu, K. (1995b). Analytic and semi-analytic solutions in electrical impedance tomography: II. Three-dimensional problems. *Physiological Measurements, 16*, 91–110.

Scharfetter, H., Merwa, R., & Pilz, K. (2005). A new type of gradiometer for the receiving circuit of magnetic induction tomography (MIT). *Physiological Measurement, 26*, S307–S318.

Soni, N. K., Paulsen, K. D., Dehghani, H., & Hartov, A. (2006). Finite element implementation of Maxwell's equations for image reconstruction in electrical impedance tomography. *IEEE Transactions on Medical Imaging, 25*(1), 55–61.

Swisstom AG. http://www.swisstom.com/.

Talmor, D., Sarge, T., Malhotra, A., O'Donnell, C. R., Ritz, R., Lisbon, A. et al. (2008) Mechanical ventilation guided by esophageal pressure in acute lung injury. The New England Journal of Medicine 359:2095–2104.https://doi.org/10.1056/NEJMoa0708638.

Tidswell, A. T., Gibson, A., Bayford, R. H., & Holder, D. S. (2001). Three-dimensional electrical impedance tomography of human brain activity. *NeuroImage, 13*, 283–294.

Wolf, G. K., & Arnold, J. H. (2006). Electrical impedance tomography: Ready for prime time? *Intensive Care Medicine, 32*, 1290–1292. https://doi.org/10.1007/s00134-006-0253-z

Wu, Y., Langlois, P. J., Bayford, R., & Demosthenous, A. (2016). Design of a CMOS active electrode IC for wearable electrical impedance tomography systems. ISBN Information: Electronic ISSN: 2379-447X. INSPEC Accession Number: 16226602. doi: https://doi.org/10.1109/ISCAS.2016.7527373.